

Physical, Social, and Biological Attributes for Improved Understanding and Prediction of Wildfires: FPA FOD-Attributes Dataset

Yavar Pourmohamad^{1,8}, John T. Abatzoglou², Erin J. Belval³, Erica Fleishman⁴, Karen Short⁵, Matthew C. Reeves⁵, Nicholas Nauslar⁶, Philip E. Higuera⁷, Eric Henderson⁸, Sawyer Ball⁸, Amir AghaKouchak⁹, Jeffrey P. Prestemon¹⁰, Julia Olszewski⁵, Mojtaba Sadegh^{1,11*}

¹ Department of Civil Engineering, Boise State University, Boise, ID, USA.

² Management of Complex Systems Department, University of California, Merced, CA, USA.

³ USDA Forest Service, Rocky Mountain Research Station, Fort Collins, CO, USA.

⁴ College of Earth, Ocean, and Atmospheric Sciences, Oregon State University, Corvallis, OR, USA.

⁵ USDA Forest Service, Rocky Mountain Research Station, Missoula, Montana, USA.

⁶ Bureau of Land Management, Boise, ID, USA.

⁷ Department of Ecosystem and Conservation Sciences, University of Montana, Missoula, MT, USA.

⁸ Department of Computer Science, Boise State University, Boise, ID, USA.

⁹ Department of Civil and Environmental Engineering, University of California, Irvine, CA, USA.

¹⁰ USDA Forest Service, Southern Research Station, Research Triangle Park, NC, USA.

¹¹ United Nations University Institute for Water, Environment and Health, Hamilton, ON, Canada.

* Correspond to: mojtabasadegh@boisestate.edu

Abstract

Wildfires are increasingly impacting social and environmental systems in the United States. The ability to mitigate the adverse effects of wildfires increases with understanding of the social, physical, and biological conditions that co-occurred with or caused the wildfire ignitions and contributed to the wildfire impacts. To this end, we developed the FPA FOD-Attributes dataset, which augments the sixth version of the Fire Program Analysis-Fire Occurrence Database (FPA FOD v6) with nearly 270 attributes that coincide with the date and location of each wildfire ignition in the United States. FPA FOD v6 contains information on location, jurisdiction, discovery time, cause, and final size of >2.3 million wildfires from 1992-2020 in the United States. For each wildfire, we added physical (e.g., weather, climate, topography, infrastructure), biological (e.g., land cover, normalized difference vegetation index), social (e.g., population density, social vulnerability index), and administrative (e.g., national and regional preparedness level, jurisdiction) attributes. This publicly available dataset can be used to answer numerous questions about the covariates associated with human- and lightning-caused wildfires. Furthermore, the FPA FOD-Attributes dataset can support descriptive, diagnostic, predictive, and prescriptive wildfire analytics, including development of machine learning models. The FPA FOD-Attributes dataset is available at <https://zenodo.org/record/8381129> (Pourmohamad et al. 2023).

41 **1. Introduction**

42 Wildfire (hereafter, fire) hazards have increased across many regions of the world in recent
43 decades, increasing the burden on fire prevention and suppression efforts (Alizadeh et al.,
44 2021; Modaresi Rad et al., 2023; Rad et al., 2023). Climatic changes in the past several
45 decades have generally decreased the fire season moisture content of living and dead
46 vegetation, lengthened the fire season, and contributed to a marked increase in the number of
47 critical fire danger days across much of the United States with distinct geographical and
48 seasonal trends and patterns (Westerling, 2016; Dennison et al., 2014; Bowman et al., 2011;
49 Alizadeh et al. 2023). These changes have overlapped with the impacts of decades long fire
50 suppression policies in the United States that resulted in anthropogenic fire deficits, and
51 increased fuel loads in many regions, especially low-elevation forests in the western United
52 States (Bowman et al., 2009). Human-caused ignitions compound the fire burden, particularly
53 near the wildland-urban interface (WUI), where wildlands intermingle with human
54 settlements (Stephens et al., 2013; Committee, 2013). Moreover, increases in the area and
55 density of human settlement and infrastructure in the WUI have further increased exposure to
56 fire hazards across the United States (Scott et al., 2012). The intersection of changes in the
57 number and timing of ignitions and changing environmental conditions has resulted in several
58 fires that caused substantial loss of life (e.g., Miller and Ager, 2012).

59 Studies have focused on understanding the patterns and drivers of human-caused ignitions
60 given the potential for reducing the number of such ignitions and the negative impacts
61 associated with the resulting fires, particularly near the WUI (Short, 2014; Balch et al., 2017).
62 The primary factors that are often included in models of human-caused ignitions are social
63 and economic (e.g., demographics), environmental (e.g., vegetation, meteorology,
64 topography), anthropogenic (e.g., land ownership, distance to roads), and timing metrics (e.g.,
65 holidays, weekends) (Short, 2022). Similarly, advances in predictive understanding of
66 lightning-ignited fires have improved the speed and effectiveness of suppression responses
67 (Ronchi et al., 2017; McGee et al., 2015). Fuel moisture (Viegas et al., 1992; Meisner et al.,
68 1993; Pineda et al., 2022), vegetation type and condition (Dissing and Verbyla, 2003;
69 Wierzchowski et al., 2002), weather (Wierzchowski et al., 2002; Hély et al., 2001), pre-fire-
70 season snowpack (Chen and Jin, 2022), duration of lightning contact with fuel (Fuquay et. al.,
71 1979; Latham and Williams, 2001), number of lightning strikes (Flannigan and Wotton,
72 1991), and topography (Hessilt et al., 2022) are the main cited factors that affect natural fires.
73 However, the confluence of factors that shape spatial and temporal patterns of ignitions,
74 especially human-caused ignitions, confounds efforts to predict, prevent, and prepare for the
75 impacts of fires.

76 The most comprehensive source of georeferenced fire ignition data in the United States is the
77 Fire Program Analysis Fire Occurrence Database (Short, 2014), which aggregates fire reports
78 from federal, state, and local entities with fire protection and reporting responsibilities. All
79 fires in the FPA FOD database are referenced to a discovery date, final fire size (area within

80 the fire perimeter), and a point location at least as precise as a Public Land Survey System
81 section (i.e., 1 square mile grid). Most fire records are also associated with attributes
82 including fire name, discovery time, reporting agency information, ignition cause, and
83 containment date and time. The 13 cause classes, as determined by the reporting agency, are
84 natural; recreation and ceremony; equipment and vehicle use; debris and open burning;
85 smoking, arson or incendiarism; railroad operations and maintenance; misuse of fire by a
86 minor; power generation, transmission, or distribution; fireworks, firearms and explosives
87 use; other causes; and missing data, not specified, or undetermined (Short, 2021). FPA FOD
88 also includes incident identification numbers that can be referenced to other fire databases,
89 such as Monitoring Trends in Burn Severity (Eidenshink et al., 2007) and All-hazards dataset
90 (St. Denis et al., 2023). The sixth version of FPA FOD includes more than 2.3 million fire
91 records that correspond to a total of more than 72.8 million ha (180 million acres) burned
92 from 1992-2020 across the United States (Short, 2022).

93 To enable stronger inferences about factors that affect and predict fire ignitions and
94 outcomes, we augmented the sixth version of FPA FOD (FPA FOD v6) with 267 attributes
95 associated with the date and location of ignition across the United States. Major classes of
96 these attributes encompass climate, weather and fire danger, topography, land cover and
97 vegetation, jurisdiction and management, infrastructure, and social context. Although the
98 attributes are associated with the date and point of ignition, we also included summary
99 statistics within a temporal buffer (e.g., 5 days centered on the ignition date) and a spatial
100 buffer (e.g., 1 km) around the ignition point. Additionally, we included monthly, satellite-
101 derived vegetation indices during the 12 months prior to the ignition. The resultant FPA
102 FOD-Attributes dataset includes a total of 310 attributes associated with more than 2.3
103 million fire incidents across the United States from 1992-2020. This rich, tabular dataset can
104 be used in a variety of hypothesis-driven or data-exploration applications.

105 **2. Methods**

106 **2.1. Data Sources**

107 The FPA FOD-Attributes dataset brings together 267 attributes associated with fire ignitions
108 from 24 data sources (Tables 1 and S1). The accuracy, precision, and uncertainty of each
109 attribute, including spatial and temporal resolution, depends on the source data. Availability
110 of attributes for individual fire incidents also depends on the spatial and temporal coverage of
111 the source data. Table 1 lists general categories of attributes, their resolution and coverage,
112 and their sources. Table S1 lists more detail about individual attributes that are included in
113 the FPA FOD-Attributes dataset.

114 Source data were either in raster or vector/point formats. For raster data, we selected the
115 attribute value of the grid cell that contained the ignition point recorded in the FPA FOD
116 dataset. Similarly, for vector/shapefile formatted data, we selected the attribute value of the
117 area associated with the ignition point. When distance from the fire location to a vector was
118 of interest, we estimated the nearest perpendicular distance. We conducted all analyses with
119 Python libraries xarray and GDAL (raster data) or GeoPandas (vector data). Source code is

120 provided along with the FPA FOD-Attributes dataset to support future use (see Code
 121 Availability and Data Availability sections).

122 Table 1. Variables in the FPA FOD-Attributes dataset and their data sources. See Table S1
 123 for a detailed description of all variables and sources.

	Variable category	Spatial resolution	Temporal resolution	Temporal extent	Spatial extent	Source
Weather and climate	Weather and fire danger	~4 km	Daily	1979-present	CONUS	gridMET (Abatzoglou, 2013)
	Climate normal	~4 km	Daily	1990-2020	CONUS	gridMET
	Climate percentiles	~4 km	Daily	1990-2020	CONUS	gridMET
Land cover and topography	Omernik ecoregions level II and III	Vector	Static	NA*	North America	EPA*
	Pyrome	Vector	Static	NA	CONUS	Short, 2022
	Topography	30 m	Static	NA	U.S.	USGS et al., 2023
	Existing vegetation	30 m	Periodic	2001, 2012, 2014, 2016, 2020	U.S.	USGS et al., 2023
	Fire regime group type	30 m	Periodic	2001, 2012, 2014, 2016, 2020	U.S.	USGS et al., 2023
	Normalized Difference Vegetation Index (NDVI)**	5.60 km	16 days	2000-present	Global	Didan, 2021
	NDVI**	5.55 km	Daily	1981-present	Global	Vermote, 2019
	Land cover	33.3 m	Periodic	1992, 2001, 2004, 2006, 2008, 2011, 2013, 2016, and 2019	U.S.	Dewitz, 2019
	Rangeland production	30 m	Annual	1984-2021	Rangelands across CONUS	Reeves and Frid, 2016
	Exotic annual and native perennial grasses	30 m	Annual	2016-2021	Extended Western U.S.	USGS, 2023
Social	Climate and economic justice screening tool	Census tract	Static	2010	U.S.	Climate and Economic Justice Screening Tool, 2023
	Social vulnerability index	Census tract	Periodic	2000, 2010, 2014, 2016, 2018, and 2020	U.S.	Flanagan et al., 2018
	Population density	100 m	Annual	2000-present	Global	WorldPop, 2018
	Gross domestic product	9.3 km	Periodic	1990, 2000, 2015	Global	Kummu et al., 2018
	Global human modification	1 km	Static	NA	Global	Kennedy et al., 2019
Administrative	Risk management assistance	30 m	Static	NA	CONUS	Silva et al., 2020
	Fire Stations	Point	Static	NA	U.S.	Fire Stations, 2023
	GACC preparedness level	GACC	Daily	2007-2021	U.S.	Nguyan et al., 2023
	National preparedness level	National	Daily	1990-present	U.S.	Wildland fire perimeters full history, 2023

	Conservation status	Vector	Static	NA	U.S.	USGS, 2022
	Distance to road	Vector	Static	NA	U.S.	TIGER: US Census Roads

124

125 *EPA: U.S. Environmental Protection Agency – MODIS: Moderate Resolution Imaging
 126 Spectroradiometer – USGS: U.S. Geological Survey – NASA: National Aeronautics and
 127 Space Administration – NOAA: National Oceanic and Atmospheric Administration –
 128 NLCD: National Land Cover Dataset – CDC: Centers for Disease Control and Prevention –
 129 GACC: Geographic Area Coordination Center – NIFC: National Interagency Fire Center –
 130 SEDAC: Socioeconomic Data and Applications Center – TIGER: Topologically Integrated
 131 Geographic Encoding and Referencing – NA: Not Applicable – CONUS: contiguous United
 132 States

133 **NDVI from Didan, 2021 provides monthly mean vegetation health information for the 12
 134 months prior to fire, whereas that from Vermote, 2019 offers NDVI value in the day prior to
 135 fire start date as well as daily mean, max, and min NDVI for each month within one year
 136 prior to fire.

137 2.2. Data Compilation

138 Here, we briefly discuss the data compilation process and assumptions. Table S1 provides a
 139 detailed description of the variables, their units, and sources. Unless otherwise specified, the
 140 FPA FOD-Attributes dataset provides a complete record of values of each variable for all fire
 141 events from 1992-2020.

142 2.2.1. Weather and climate

143 Our main source of weather and climate data was gridMET (Abatzoglou, 2013), which
 144 merged gridded climate and reanalysis data with gauge-based precipitation data to provide
 145 spatially and temporally complete, high-resolution (4 km) gridded data on surface
 146 meteorological variables. gridMET also provides daily fire danger indices based on Fuel
 147 Model G from the National Fire Danger Rating System 77 (Cohen and Deeming, 1985).
 148 gridMET is widely used in fire-related studies (Alizadeh et al., 2021, 2023).

- 149 ● Weather and fire danger indices

150 Attributes associated with each fire ignition in the FPA FOD-Attributes dataset include daily
 151 precipitation, maximum and minimum temperature (2 m above ground), relative humidity,
 152 specific humidity, wind velocity (10 m above ground), surface downward shortwave
 153 radiation, reference evapotranspiration, and vapor pressure deficit; all data are for the date
 154 and point of fire ignition. We also derived the following fire danger indices for the date and
 155 point of fire ignition: 100-hour and 1000-hour dead fuel moisture, energy release component
 156 (ERC), and burning index (BI). ERC and BI are fuel model dependent, and hence are aligned
 157 with a single fuel model (Model G – dense coniferous forest fuel type), but 100-hr and 1000-
 158 hr dead fuel moisture variables are fuel model agnostic. Additionally, we derived maximum,
 159 minimum, and average values of these variables within a 5-day window centered on the fire

160 ignition date (i.e., from 2 days prior to 2 days after the ignition date). This arbitrary selection
161 is to allow additional analyses, especially for fires associated with uncertainty in
162 detection/reporting of start dates.

163 • Climate normals

164 A climate normal is defined as the long-term (1990-2020) average of daily surface
165 meteorological variables. Climate normals characterize average weather conditions. The
166 attributes include climate normals of all meteorological and fire danger indices listed above
167 for the location and day of year of fire ignition.

168 • Climate percentiles

169 We calculated the percentile range for meteorological and fire danger indices for the location
170 and the day of year of fire ignition, relative to values from the same day of the year from
171 1979-2020. The percentile range enables the user to compare the attribute with long-term
172 records. We report the data in discrete ranges of <10th, 10th -30th, 30th -50th, 50th -70th, 70th -
173 90th, and >90th. Depending on the attribute, a higher percentile range might be associated with
174 higher (e.g., ERC) or lower (e.g., 1000-hr dead fuel moisture) fire danger.

175 **2.2.2. Land cover and topography**

176 We used data from the U.S. Forest Service (USFS), U.S. Geological Survey (USGS),
177 LANDFIRE, National Oceanic and Atmospheric Administration (NOAA), National
178 Aeronautics and Space Administration (NASA), and U.S. Environmental Protection Agency
179 (EPA) to derive attributes associated with land surface conditions at the location and time of
180 fire ignition. We provide multiple land-cover data sources to allow users to select the source
181 that best suits their needs.

182 Given the potential biases in reporting of the ignition location, statistics of variables within a
183 1-km radius around the ignition location, especially variables derived from 30-m or other
184 fine-resolution products, are likely a more accurate representation of the ground conditions
185 than values specifically at the point of ignition. For fires that burn large areas, note that land
186 cover can vary widely and thus may differ from that at the point of ignition,

187 • Omernik ecoregions

188 Ecoregions denote areas with similar biotic and abiotic attributes (Omernik, 1987). Ecoregion
189 shapefiles (i.e., vector data) are available at four levels: 15 Level 1 ecoregions, 50 Level 2
190 ecoregions, and 182 Level 3 ecoregions across North America, and 967 Level 4 ecoregions in
191 the CONUS. Many fire-related studies used Level II or III ecoregions (Dennison et al., 2014;
192 Alizadeh et al., 2021, 2023), and we provide these two ecoregion classifications at the
193 ignition point of each fire.

194 • Pyrome

195 Pyromes are regions with relatively homogeneous contemporary fire regimes (e.g., start and
196 end date of fire season, frequency of fire, modality and large-fire size); 128 pyromes have

197 been identified in CONUS (Short et al., 2020). We provide the pyrome associated with the
198 ignition point of each fire.

199 • Topography

200 Topography affects the likelihood of fire ignition and fire behavior. We derived elevation,
201 slope, aspect, the Topographic Position Index (TPI), and Terrain Ruggedness Index (TRI).
202 Positive and negative TPI values represent locations that are higher and lower, respectively,
203 than their neighboring grid cells (Weiss, 2001). TRI indicates the magnitude of elevation
204 change between neighboring grid cells (Riley et al., 1999). We derived elevation (above
205 mean sea level), slope, and aspect from LANDFIRE products (30-m resolution). We derived
206 TPI and TRI from the LANDFIRE digital elevation model with the GDAL library in Python.
207 The FPA FOD-Attributes dataset includes these variables at the fire ignition point, and also
208 averaged across a 1-km radius around the fire ignition point.

209 • Existing vegetation

210 We used Existing Vegetation Cover (EVC), Existing Vegetation Height (EVH), and Existing
211 Vegetation Type (EVT) data from LANDFIRE (30-m resolution) to represent vegetation as
212 close as possible to the point and date of fire ignition. EVC, EVH, and EVT are available for
213 2001, 2012, 2014, 2016 and 2020. For each fire ignition, we used the most recent prior data
214 product. For all fires prior to 2001, we used the 2001 product. We used the codes for
215 vegetation variables as in the original dataset (<https://landfire.gov/vegetation.php>). We also
216 report the most frequently occurring EVC, EVH, and EVT classification within a 1-km radius
217 around each fire ignition point.

218 • Fire regime group

219 Fire regime group (FRG) characterizes the presumed historical fire regime in a given
220 location. We report the most frequently occurring FRG within the 1-km radius around each
221 ignition point, for the prior year closest to the date of ignition. Data on FRG are available
222 through LANDFIRE for 2001, 2012, 2014, and 2016. We used the 2001 product for all
223 ignitions prior to 2001. FRG codes in FPA FOD-Attributes correspond to those in
224 LANDFIRE (<https://landfire.gov/CSV/FRG.csv>).

225 • Normalized Difference Vegetation Index (NDVI) and Enhanced Vegetation Index
226 (EVI) from NASA's MODIS sensor

227 NDVI is an index of vegetation greenness (Rouse et al., 1974) that is closely related to
228 primary productivity and leaf cover. EVI is a similar index that generally is more accurate in
229 regions with high vegetation biomass (Huete et al., 2002). We obtained NDVI and EVI from
230 NASA's MOD13C2 v6.1 product (5.6 km resolution), which provides monthly NDVI and
231 EVI indices from 2000 to present. We derived NDVI and EVI at the point of ignition in the
232 month prior to the ignition date and the 11 previous months. The FPA FOD-Attributes dataset
233 does not include NDVI and EVI values for ignitions prior to 2000.

234 • NDVI from NOAA

235 We also obtained NDVI from NOAA’s daily gridded NDVI product (5.55 km resolution),
236 which was derived from the Surface Reflectance Climate Data Record based on Advanced
237 Very High Resolution Radiometer (AVHRR) and Visible Infrared Imaging Radiometer Suite
238 (VIIRS) images (Vermote, 2019). We acquired the NDVI value associated with the location
239 of ignition on the day prior to the fire discovery date. FPA FOD-Attributes also includes
240 monthly mean, maximum, and minimum NDVI for the 12 months prior to the ignition date.

241 • Land cover

242 We used the National Land Cover Database (NLCD) to derive the most recent prior land-
243 cover type associated with each point and date of fire ignition. These data are similar to EVC,
244 and users may opt to select one or the other. NLCD data are available for 1992, 2001, 2004,
245 2006, 2008, 2011, 2013, 2016, and 2019. Land cover classes and the method used to classify
246 land cover from Landsat images differed between 1992 and all other years (Dewitz, 2019).
247 The attributes include land-cover type at the point of ignition and the three land-cover types
248 with the greatest percentage of cover within a 1-km radius around the ignition point.

249 • Rangeland production

250 The rangeland production metric quantifies annual plant biomass production on 268 million
251 hectares (662 million acres) of rangeland across the CONUS from 1984 to present at 30 m
252 resolution. We derived rangeland production values at the ignition point and within a 1-km
253 radius around the ignition point for the year of fire. Values of rangeland production are only
254 provided for ignitions within the domain of the Rangeland Production Monitoring Service
255 (Reeves et al., 2021).

256 • Exotic annual and native perennial grasses

257 We used annual fractional cover maps (30-m resolution) for (1) a group of 17 exotic annual
258 grasses, (2) cheatgrass (*Bromus tectorum*), (3) medusahead (*Taeniatherum caput-medusae*),
259 and (4) Sandberg bluegrass (*Poa secunda*) from 2016-2021 (USGS, 2023). These data are
260 generated from on-the-ground observations by the U.S. Bureau of Land Management and
261 application of a machine learning model to Harmonized Landsat and Sentinel images (Dahal
262 et al., 2022). The FPA FOD-Attributes dataset provides percent cover for each of the four
263 above-mentioned categories of grasses on the date and for the location of ignition from 2016-
264 2020, within the spatial domain of the source data (extended western United States).

265 **2.2.3. Social and economic context**

266 We used a variety of government and academic data sources to derive social and economic
267 attributes associated with the location of fire ignitions. Many of these sources are based on
268 the United States or, in some cases, global census data.

269 • Climate and economic justice screening tool

270 We used the U.S. Council on Environmental Quality’s Climate and Economic Justice
271 Screening Tool (CEJST) v.0 to derive metrics associated with community-level burdens

272 related to climate change, energy, health, housing, legacy pollution, transportation, water and
273 wastewater, and workforce development. Because values of CEJST’s 107 variables currently
274 are static, we assigned values to all fire ignitions in the entire period of record on the basis of
275 location. CEJST is derived from 2010 U.S. census data and values of variables are available
276 at the tract level. CEJST classifies a community as disadvantaged if it is “(1) at or above the
277 threshold for one or more environmental, climate, or other burdens, and (2) at or above the
278 threshold for an associated socioeconomic burden” (<https://screeningtool.geoplatform.gov/>).

279 • Social vulnerability index

280 We used the U.S. Centers for Disease Control and Prevention’s nested hierarchical social
281 vulnerability index (SVI), which provides a measure of vulnerability for each census tract in
282 terms of overall vulnerability, four general dimensions of vulnerability (socioeconomic
283 status, household composition and disability, housing type and transportation, minority status
284 and language), and 15 subdimensions of vulnerability (e.g., income, age, minority, no
285 vehicles). Values of the SVI range from 0 (low vulnerability) to 1 (high vulnerability). SVI
286 estimates are available for 2000, 2010, 2014, 2016, 2018, and 2020. The FPA FOD-
287 Attributes dataset includes the overall SVI value and values of the dimensions and
288 subdimensions of vulnerability for the location and year of each fire ignition. We used the
289 most recent SVI prior to the ignition date. We assigned vulnerability attributes to ignitions
290 prior to 2000 from the 2000 SVI data.

291 • Population density

292 We obtained population density and its average within a 1-km radius around the point of
293 ignition from the WorldPop dataset (Tatem, 2017), which provides annual global population
294 data from 2000-present at 100-m resolution. We did not assign a population density value to
295 fire ignitions prior to 2000.

296 • Gross domestic product

297 We derived per capita gross domestic product (GDP) at the location of each ignition in the
298 most recent year prior to the ignition date. Our global data source (Kummu et al., 2018)
299 provides subnational GDP per capita for 1990, 2000, 2015 at 5 arc-min resolution.

300 • Global human modification

301 We assigned a static global human modification (GHM) index, which indicates the
302 cumulative human modification of lands, to each fire ignition on the basis of its location. We
303 derived GHM values from data provided by the NASA Socioeconomic Data and Applications
304 Center (1-km resolution at the global level), which were originally developed by (Kennedy et
305 al., 2019).

306 **2.2.4. Administrative**

307 We used a variety of data sources, mostly from the U.S. government, to acquire attributes
308 associated with management.

309 • Risk management assistance program

310 We used the two static, raster-formatted risk maps provided by the Risk Management
311 Assistance program to acquire evacuation time from the fire ignition location to a medical
312 care facility and the suppression difficulty index (SDI; Silva et al., 2020) for the fire ignition
313 point. SDI is a measure of relative difficulty of fire control given topography, fuels, expected
314 severe weather fire behavior, firefighter line production rates in various vegetation types, and
315 accessibility (e.g., distance from roads or trails).

316 • Fire stations

317 We derived the number of fire stations within a 1-, 5-, 10-, and 20-km radius around each fire
318 ignition point. The location of fire stations comes from the static Homeland Infrastructure
319 Foundation-Level Data.

320 • Geographic area coordination centers (GACC) preparedness level

321 The nine GACCs in CONUS also have preparedness levels that are based on the regional
322 availability of wildland firefighting resources and fire activity. We obtained the GACC
323 preparedness level for all fire ignitions over the period 2007-2020 (Nguyan et al., 2023). Data
324 are not available for fire ignitions prior to 2007.

325 • National preparedness level (NPL)

326 National preparedness level indicates suppression resource availability for emerging fires on
327 the basis of fuel and weather conditions, current fire activity, and resource commitments;
328 there is a single NPL reflecting the entire nation. We acquired the NPL associated with the
329 date of all fire ignitions from the National Interagency Fire Center (NIFC). NPLs are
330 determined by the National Multiagency Coordination Group or the National Interagency
331 Coordination Center (NICC) daily during the fire season and are published by NICC as a part
332 of the daily Incident Management Situation Report (IMSR; Nguyan et al., 2023).

333 • Conservation status

334 The Gap Analysis Project (GAP) is a USGS-based program that evaluates whether common
335 species of plants and animals are adequately protected and tracks the conservation status of
336 lands and waters nationwide. From GAP's vector-based static data, we obtained management
337 jurisdiction and agency (e.g., U.S. Fish and Wildlife Service), land management designation
338 (e.g., Wilderness Area, National Recreation Area), and GAP status code and priority (extent
339 to which conservation of biological diversity is prioritized) for all fire ignition points.

340 • Distance to road

341 We used the vector-based, static Topologically Integrated Geographic Encoding and
342 Referencing (TIGER) database to derive the minimum distance (perpendicular) from the
343 point of fire ignition to primary, secondary, local, and other roads and to all-terrain vehicle
344 and non-motorized vehicle trails.

345 **3. Data validation**

346 The FPA FOD-Attributes dataset is a derivative dataset, and hence the accuracy, precision
347 and uncertainty of the fire attributes reflect those of the source data. We selected reliable
348 source data to ensure the quality of attribute data associated with each fire. Our validation
349 process was focused on ensuring the attributes are consistent with the source. We followed
350 four steps to validate our data:

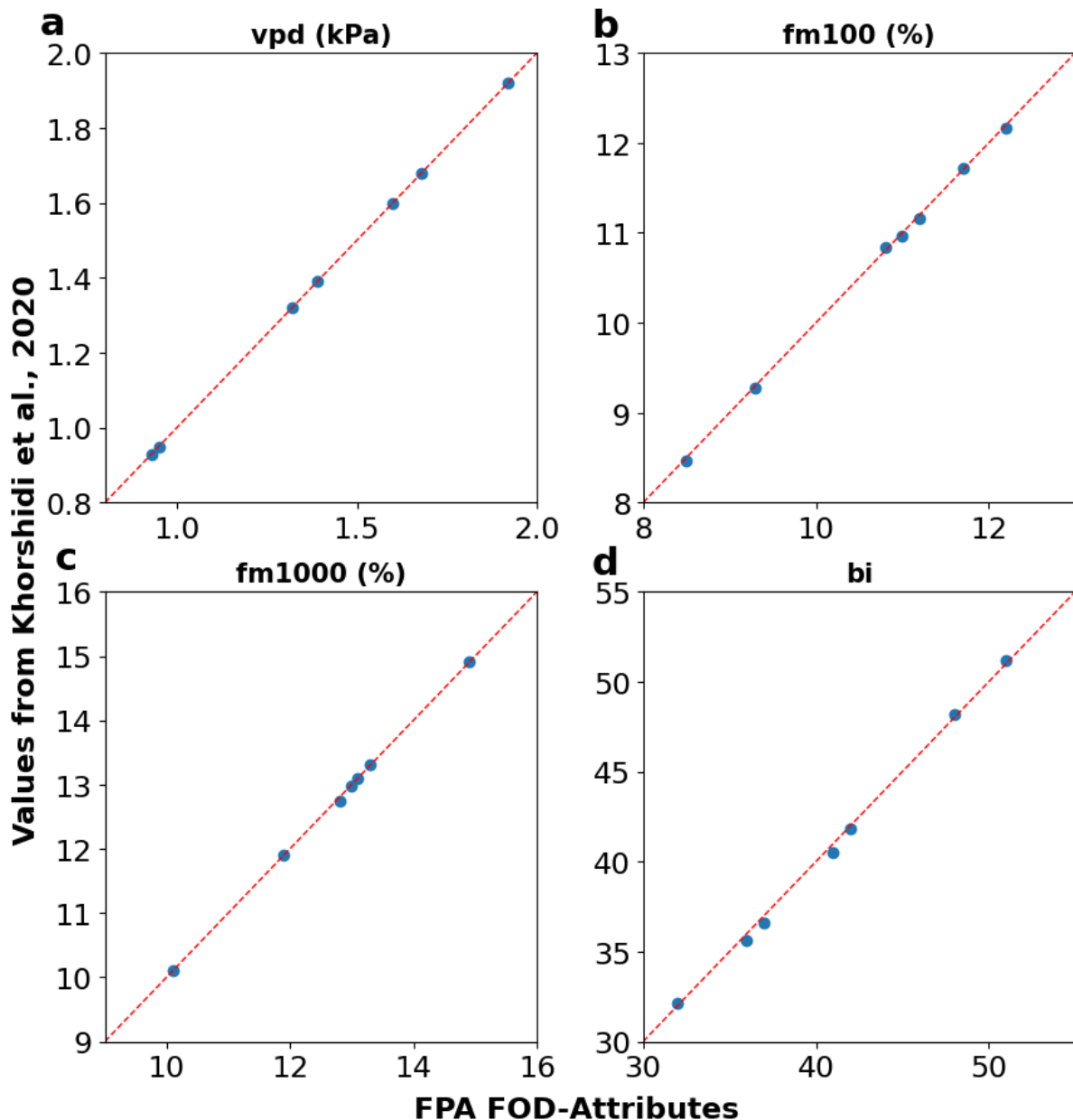
- 351 1. Manual comparison of attribute values for selected fires from the source data to those
352 in the FPA FOD-Attributes dataset.
- 353 2. Comparison of the attributes in the FPA FOD-Attributes dataset and another
354 published study.
- 355 3. Investigation of the temporal evolution of attributes associated with selected fires and
356 those in the FPA FOD-Attributes dataset.
- 357 4. Comparison of attributes from the FPA FOD-Attributes dataset with those reported by
358 the news media.

359 **3.1. Manual comparison**

360 We compared values of attributes of 100 randomly selected fires that spanned the spatial and
361 temporal domain from the FPA FOD-Attributes dataset and manually extracted source data in
362 QGIS (raster and vector-based data) or Excel (tabular data). We assumed that manual
363 comparison would detect any systematic errors in the Python code used to develop the FPA
364 FOD-Attributes dataset. All attribute values for all selected fire ignitions matched those of the
365 source data.

366 **3.2. Comparison with the literature**

367 We compared the meteorological and fire danger indices associated with seven fires in
368 Southern California listed in Table S6 of (Khorshidi et al., 2020) with those in the FPA FOD-
369 Attributes dataset. Because (Khorshidi et al., 2020) also used gridMET, we expected the two
370 sets of values to match. With the exception of rounding errors, values of vapor pressure
371 deficit (VPD), 100-hr and 1000-hr dead fuel moisture (FM100 and FM1000, respectively),
372 and burning index (BI) from the two sources matched (Figure 1, Table S2).



373

374 Figure 1. Comparison of values of meteorological and fire danger indices associated with
 375 seven fires from FPA FOD-Attributes and (Khorshidi et al., 2020).

376

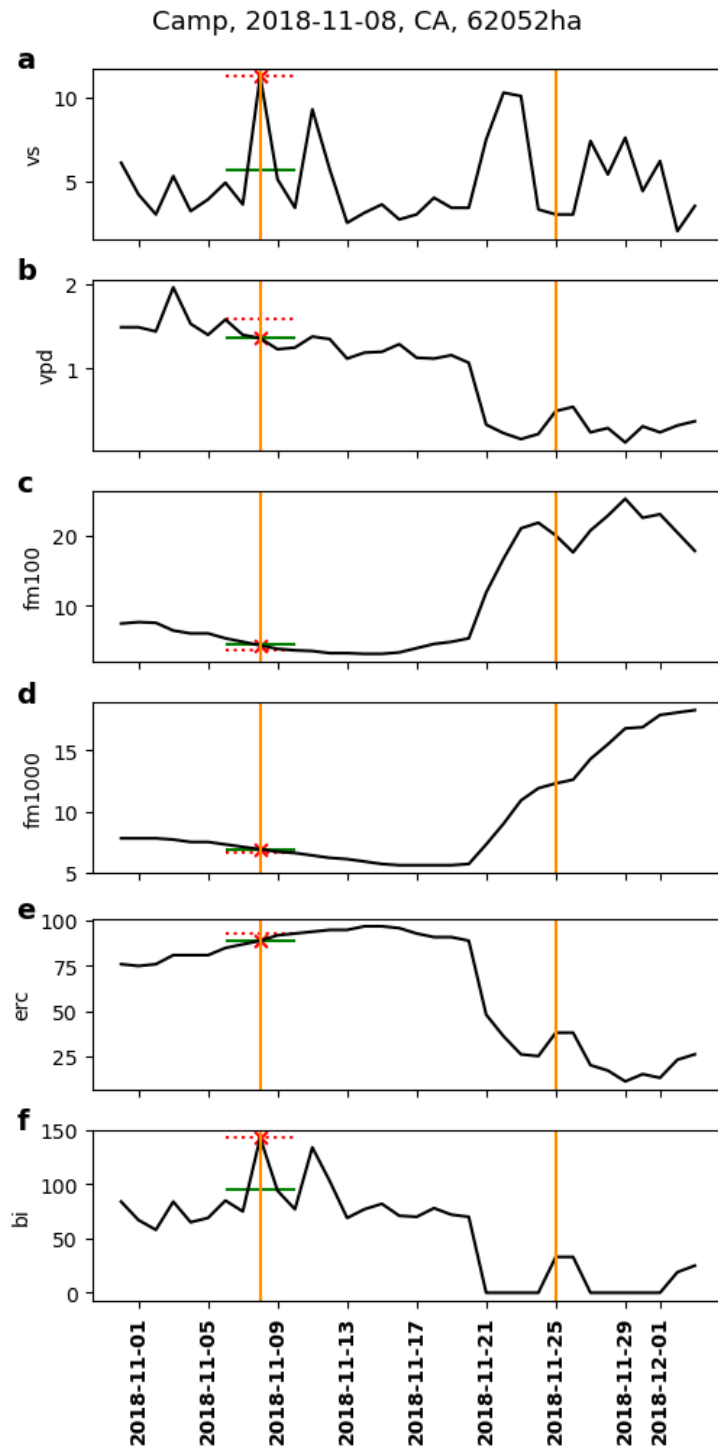
377 3.3. Temporal evolution of fire attributes

378 We analyzed the temporal evolution of meteorological and fire danger indices at the point of
 379 ignition between the fire discovery and containment dates of seven high-impact fires (Table
 380 S3, Figure 2, Figures S1-S6) distributed across CONUS. The FPA FOD-Attributes dataset
 381 provides these attributes on the ignition date and in a 5-day window centered around the
 382 ignition data. Here, we present the results for the Camp Fire, which started on November 8,
 383 2018, near Paradise, California. This fire claimed 85 lives and destroyed more than 18,000
 384 structures. Camp Fire was ignited by power transmission lines in the coniferous forests of

385 Butte County, California, and spread quickly due to strong easterly downslope winds. The
386 FPA FOD-Attributes dataset indicates that the fire was ignited in an evergreen forest (NLCD
387 classification) and that the land cover within a 1-km radius was 50% evergreen forest, 41%
388 shrub/scrub, and 6% “developed, open space”. The three most prevalent existing vegetation
389 heights within a 1-km radius of the ignition point were 18 m (trees; 43%), 38 m (trees; 23%),
390 and 0.8 m (herbaceous plants; 9% herb). These data match the official reports and news
391 accounts of the fire (e.g., Maranghides et al., 2021, and references therein). The elevation of
392 the fire ignition in the FPA FOD-Attributes dataset, 608 m, is consistent with the downslope
393 spread of the fire from the ignition point toward the city of Paradise (elevation 542 m).

394 We extracted wind velocity (VS), VPD, FM100, FM1000, energy release component (ERC),
395 and BI from late October to early December 2018 at the ignition point of the Camp Fire from
396 gridMET and the FPA FOD-Attributes dataset. Values of the two sets of variables matched
397 (Figure 2). Furthermore, the evolution of meteorological and fire danger variables followed
398 the known pattern: the Camp Fire started on a windy day (Figures 2a,f) concurrent with dry
399 vegetation (Figures 2b-e), and it was contained by the first rainstorm of the water year on
400 November 25. The arrival of the storm decreased fire danger and increased fuel moisture
401 (Figures 2b-f).

402



403

404 Figure 2. Evolution of meteorological and fire danger indices from late October to early
 405 December 2018 at the ignition point of the Camp Fire. Fire discovery and containment dates
 406 are indicated with vertical orange lines, the attribute value at the date of ignition is indicated
 407 with red asterisks, and the attributes' five-day average and maximum (VS, VPD, ERC, BI) or
 408 minimum (FM100, FM1000) values are indicated with green and red horizontal lines. VS:
 409 wind speed, VPD: vapor pressure deficit, ERC: energy release component, BI: burning index,
 410 FM100/FM1000: 100-/1000-hour dead fuel moisture.

411

412 Figures S1-S6 show the evolution of meteorological and fire danger attributes associated with
413 six additional fires across the CONUS, also providing evidence of the validity of the FPA
414 FOD-Attributes dataset.

415 **3.4. Comparison with media reports**

416 We also compared the fire attributes from the FPA FOD-Attributes dataset with media
417 accounts of two major fires, the Martin and East Troublesome fires. The 2018 Martin fire
418 burned more than 168,680 ha of shrublands and grasslands in Paradise Valley, Nevada. High
419 winds and high cover of cheatgrass are believed to have contributed to the quick spread of
420 this fire (Rothberg, 2018). The FPA FOD-Attributes dataset indicated that the prevalent land
421 cover (derived from NLCD) in a 1-km radius around the ignition point was shrub/scrub or
422 grassland/herbaceous; and that the majority of existing vegetation height (derived from
423 LANDFIRE) was 0.3 m (herbaceous), 0.2 m (herbaceous), and 0.8 m (shrubs). Furthermore,
424 land cover at the point of ignition included 21% cheatgrass and 27% other exotic annual
425 grasses, and daily average wind speed was in the 70%-90% range of historical records for the
426 day of the year, which is consistent with news reports (Rothberg, 2018). The FPA FOD-
427 Attributes dataset indicates an elevation of 1,415 m at the point of ignition, which is
428 comparable to the Paradise Valley, Nevada, elevation of 1,389 m.

429 The 2020 East Troublesome Fire burned 78,430 ha in the high elevations of the central Rocky
430 Mountains of Colorado (above 2,740 m). Low relative humidity and high winds enabled the
431 fire to spread rapidly through coniferous forest, kill two people, and destroy more than 400
432 structures (Colorado Encyclopedia, 2023). The FPA FOD-Attributes dataset indicates that
433 VPD and VS on the date of ignition were high relative to their historical range on the same
434 day of the year (80%-90% and >90%, respectively), and that the fire ignited at an elevation of
435 2,757 m. Land cover (derived from NLCD) within a 1-km radius around the ignition point
436 included evergreen forest (61%), shrub/scrub (32%), and deciduous forest (6%). Cheatgrass
437 is uncommon at such high elevations, and the FPA FOD-Attributes dataset did not assign any
438 cheatgrass cover to the ignition point. These metrics are consistent with the news records.

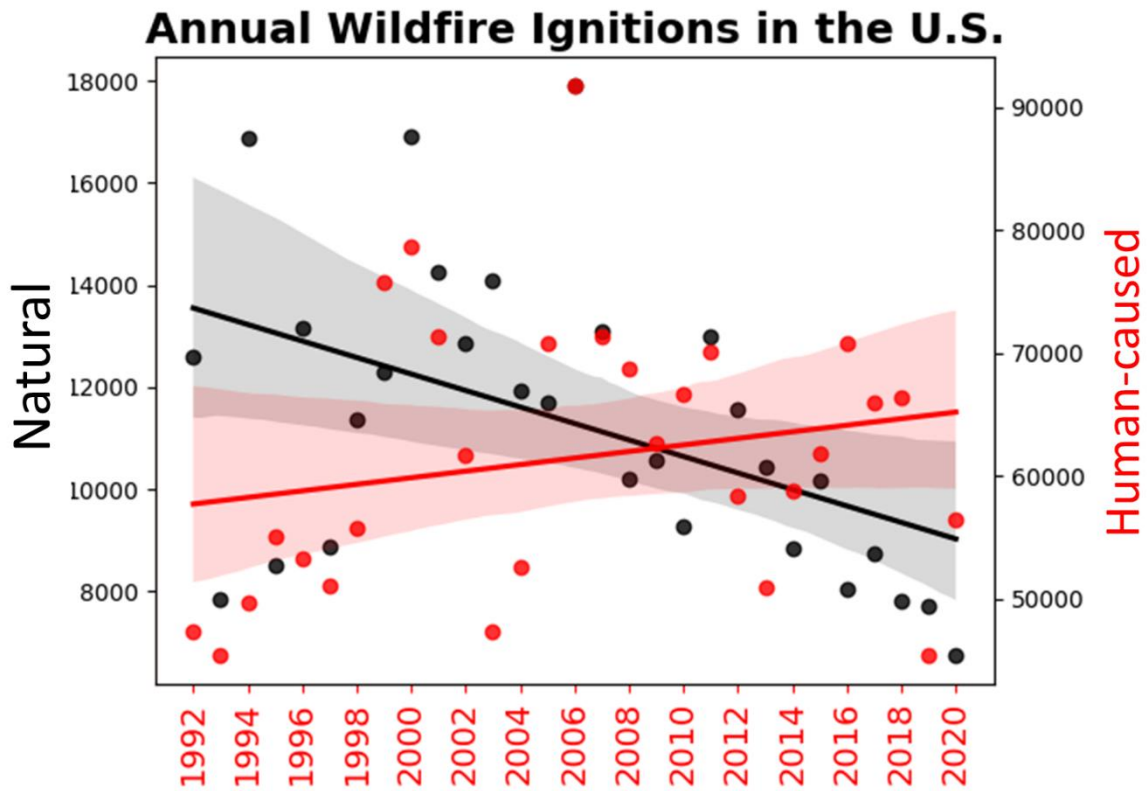
439

440 **4. Illustrative Analysis**

441 Trends and interannual variability in the number of wildfires are apparent over the 1992-2020
442 time period covered by the FPA FOD dataset. Human-caused fires increased, while lightning-
443 ignited (hereafter “natural”) fires decreased (Figure 3). Interannual variability of fire ignitions
444 is partially explained by seasonal climate and weather conditions, for example modulated
445 through fuel receptiveness to ignitions and abundance of outdoor activities (Noonan-Wright
446 et al., 2011; Finney et al., 2011). Trends are mainly attributable to fire prevention strategies
447 and climatic changes (e.g., increases in the number of critical fire danger days) (Noonan-
448 Wright et al., 2011; Khorshidi et al., 2020; Alizadeh et al., 2023). Importantly, fire ignitions
449 have temporal and spatial structures, enabling development of targeted fire prevention and
450 response strategies (Douglas et al., 2001). Figure 4, for example, shows a clear spatial pattern

451 in both human-caused and natural ignitions across the CONUS. Human-caused fires are close
452 to human settlements and roads (which can be partially explained by reporting biases; Figure
453 4a); whereas natural fires are associated with mountains in the western CONUS (Figure 4b).
454 Figures S7-S19 display the spatial distribution of ignitions associated with 13 specific fire
455 causes (natural and subcategories of human-caused fires).

456

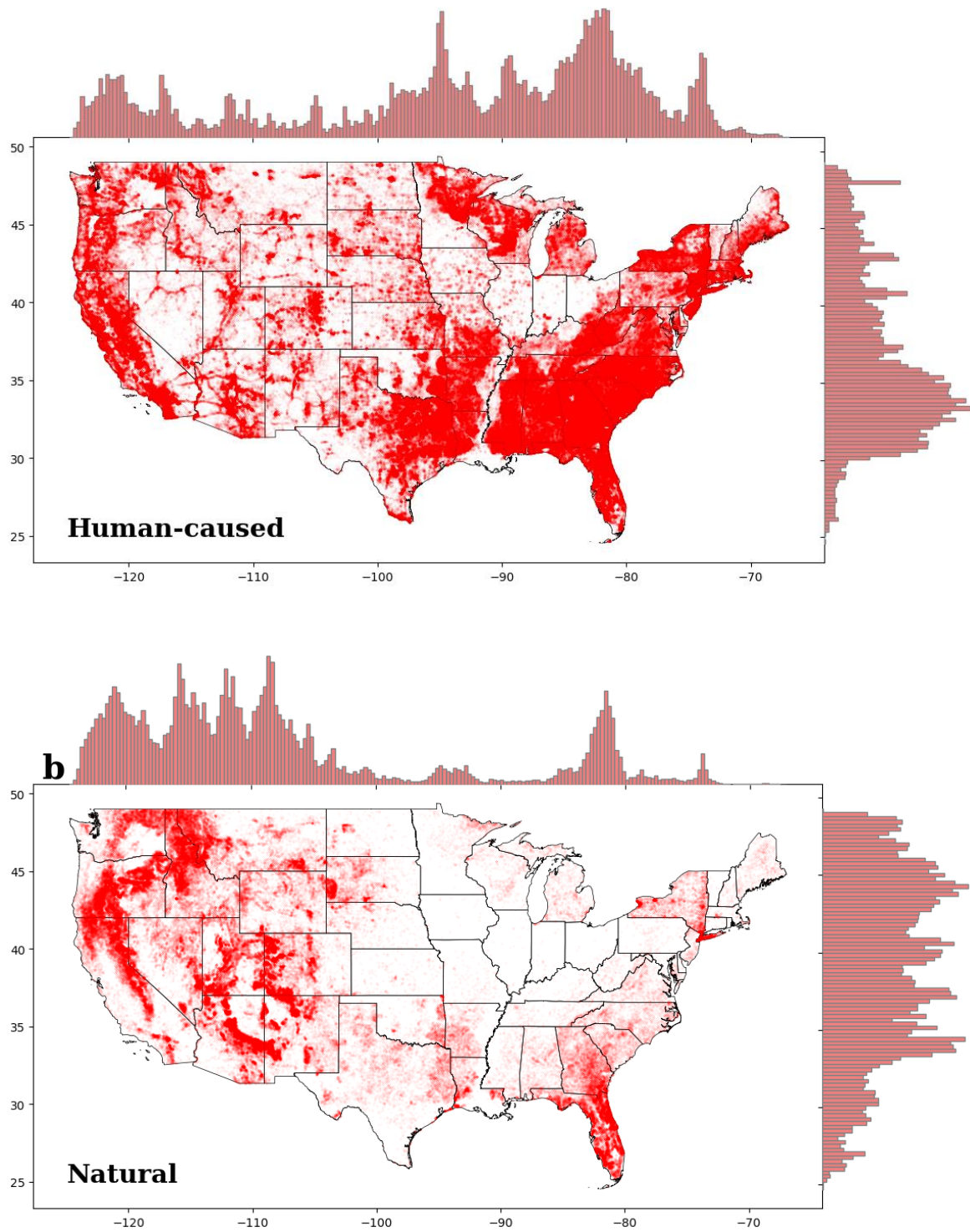


457

458 Figure 3. Trends in the annual number of natural (denoted in black) and human-caused
459 (denoted in red) fires in the contiguous United States from 1992-2020.

460

461

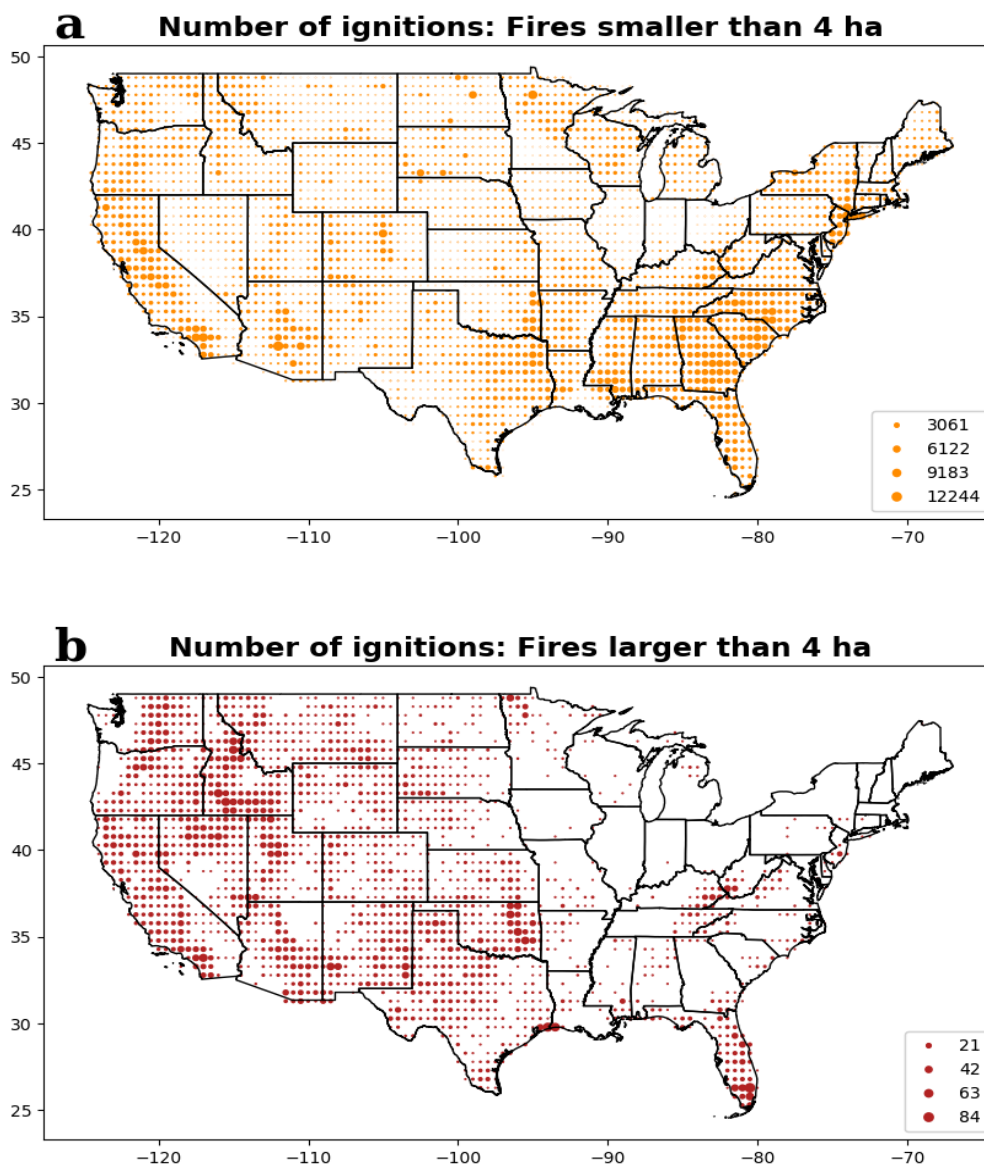


462 Figure 4. Spatial distribution of human-caused and natural fire ignitions in the contiguous
 463 United States from 1992-2020. Bars on the x- and y-axes are histograms of the longitudinal
 464 and latitudinal of ignitions, respectively.

465

466

467 We also visualized selected attributes associated with CONUS fires. Figure 5 shows the total
 468 number of fires from 1992-2020 in 0.5-degree grids across CONUS. We differentiated small
 469 fires (less than 4 ha) and large fires (greater than or equal to 4 ha). Eighty-nine percent of
 470 fires were smaller than 4 ha. Fifty-nine percent of all fires were smaller than 0.4 ha, and 97%
 471 were smaller than 40 ha, accounting for 0.08% and 2.28% of total burned area across
 472 CONUS, respectively. The number of small fires (< 4 ha) in the eastern United States and
 473 California was greater than that elsewhere in the western United States (Figure 5a). The
 474 number of fires larger than 4 ha, however, was markedly greater in the western United
 475 States, southern Great Plains, and Florida (Figure 5b).

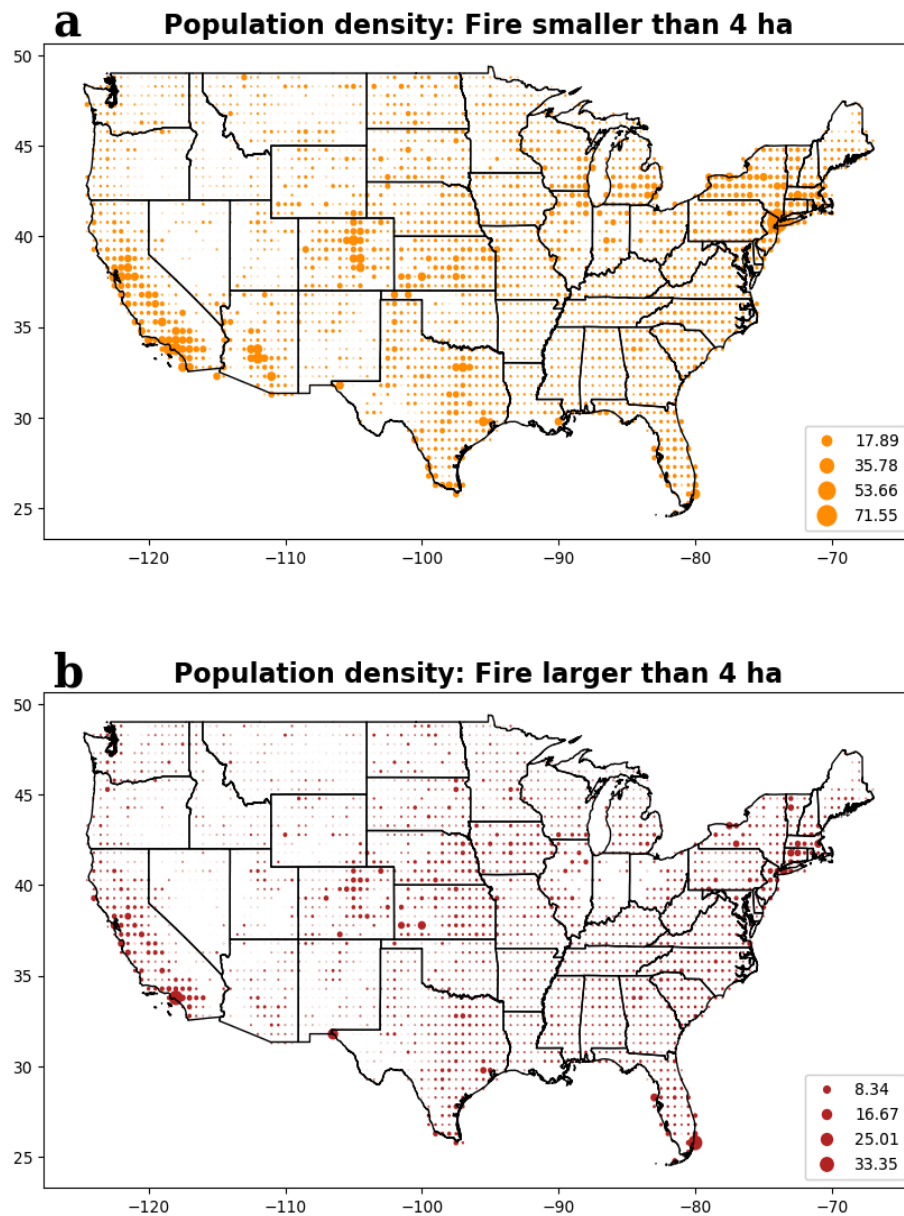


476
 477 Figure 5. Number of fires (a) less than 4 ha (10 acres) and (b) greater than or equal to 4 ha
 478 in 0.5-degree grid cells.

479

480 Small fires were associated with an average population density (2.35 people/ha; Figure
481 6a), an order of magnitude greater than that associated with large fires (0.24 people/ha;
482 Figure 6b). Fires in California, the Front Range of Colorado, and Florida were associated
483 with especially high population densities. In California, for example, small and large fires
484 were associated with population densities of 3.88 and 1.04 people/ha, respectively.
485 Furthermore, the population density associated with human-caused fires was more than
486 four times greater than that associated with natural fires (2.03 and 0.47 people/ha,
487 respectively).

488 Consistent with topography across CONUS, the average elevation of fires west of -102
489 degrees longitude was 2,146 m, compared to 1,194 m to the east. The average elevations
490 of the ignition points of natural fires were markedly higher (1,863 m) than those of
491 human-caused fires (571 m).

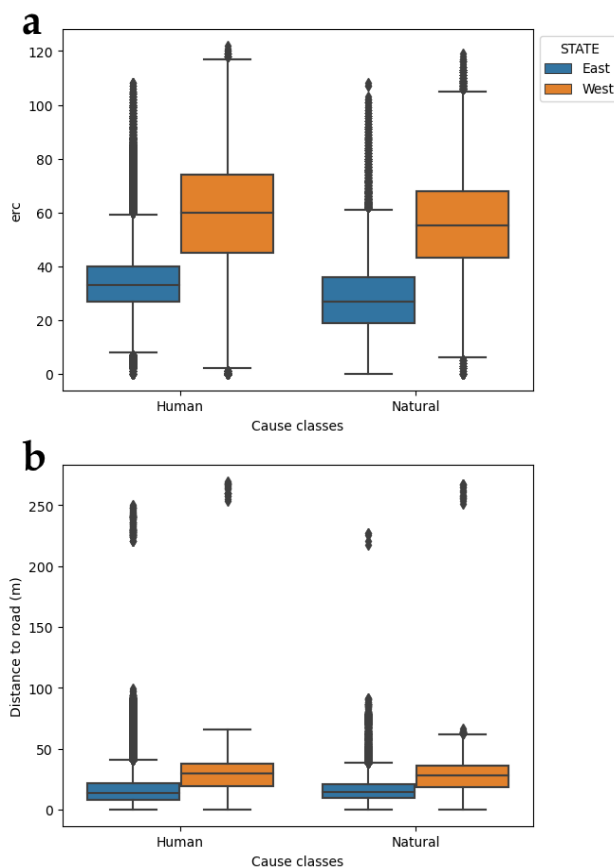


492

493 Figure 6. Average population density (people/ha) associated with fires that burned less
494 than 4 ha (a) and more than or equal to 4 ha (b) in each 0.5-degree grid cell.

495

496 Values of several attributes of fires varied along a longitudinal gradient across CONUS
497 (Figures 7-8). For example, ERC and minimum distance to the nearest road were markedly
498 greater in the western United States than in the eastern United States. Human-caused fires
499 were associated with greater ERC (60 in the western and 34 in the eastern United States)
500 than natural fires (56 in the western and 29 in the eastern United States). The minimum
501 distance to the nearest road was much lower in the eastern than western United States, which
502 is consistent with the East's higher road density and percentage of human-caused fires.
503 Minimum distance to road did not differ markedly between natural and human-caused fires
504 (Figure 7b), which likely reflects a reporting bias.



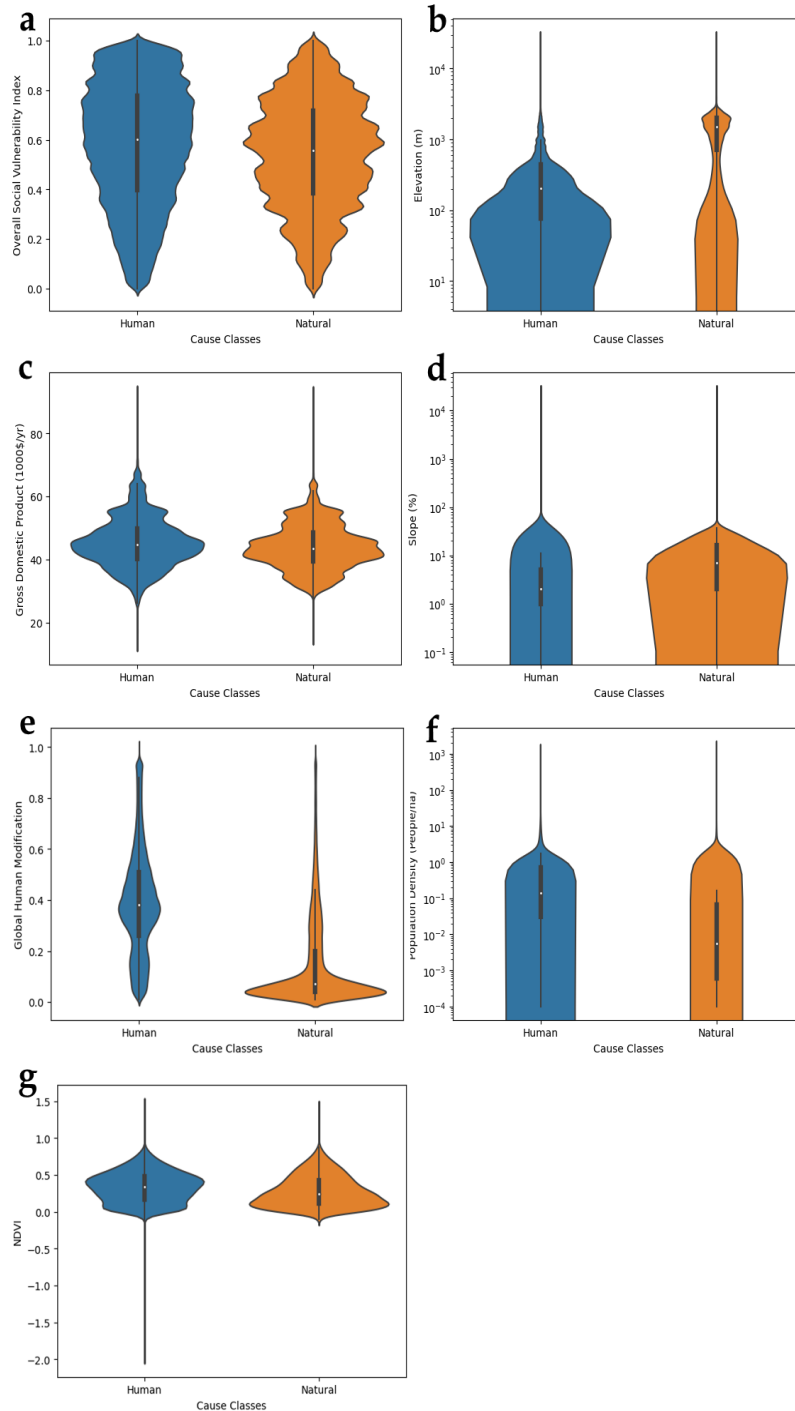
505

506 Figure 7. Boxplots of the Energy Release Component (ERC, fire danger index) (a) and
507 minimum distance to the nearest road (b) associated with human-caused and natural fires in
508 the eastern and western United States.

509

510 The elevation and slope associated with natural fires were higher than those of fires ignited
511 by human causes (Figures 8b,d). Natural fires also were associated with a lower population
512 density, normalized difference vegetation index, and global human modification index than

513 fires ignited by human causes (Figures 8e-f). Differences in the overall social vulnerability
 514 and gross domestic product associated with the ignition locations of human-caused and
 515 natural fires were less noticeable (Figures 8a,c), partly driven by the spatial resolution of the
 516 source data (Table 1).



517

518 Figure 8. Distribution of overall social vulnerability index (a), elevation (b), gross domestic
 519 product (c), slope (d), global human modification index (e), population density (f), and
 520 normalized difference vegetation index (g; one day prior to ignition date) for fires ignited by
 521 natural and human causes.

522 4. Discussion

523 Critical analysis of past fire occurrences and assessment of the success of prevention and
524 mitigation strategies are key for improving fire planning, response, adaptation, and
525 mitigation (Show and Kotok, 1923; Short, 2014). Improved understanding of the causes and
526 impacts of fires is needed to prioritize cost-effective mitigation and limit adverse fire impacts
527 (Barros et al., 2021; Houtman et al., 2013; Santos et al., 2023). Scientific advances in support
528 of fire management require comprehensive, easily accessible data that harmonize fire
529 occurrence data with potential covariates, causal factors, and associated impacts.
530 Importantly, by integrating variables that represent a range of biological, physical, and social
531 factors, the FPA FOD-Attributes dataset facilitates research that considers fire in the context
532 of social-ecological-technological systems (Iglesias et al., 2022; Shuman et al., 2022).

533 The FPA FOD-Attributes dataset includes 310 biological, physical, social, and administrative
534 attributes associated with more than 2.3 million fire records from 1992-2020 across the
535 United States. These attributes can be used for hypothesis testing and incorporation into
536 artificial intelligence and machine learning (AI-ML) models that explain drivers of past fires
537 or project likelihoods or effects of future fires. We recommend that future users carefully
538 select variables among the wealth of information provided in FPA FOD-Attributes.
539 Specifically for AI-ML modeling, variables have substantial overlap and correlation, which
540 need to be addressed. The FPA FOD-Attributes dataset potentially could be integrated with
541 satellite detection of fire starts. Satellites have been increasingly used to identify new fire
542 starts, enabling rapid deployment of suppression resources (Weaver et al., 2004; Chuvieco et
543 al., 2020). Satellite detection could be compared with the FPA FOD-Attributes dataset to
544 identify ignitions with potential to become destructive, given the surrounding conditions.
545 This information could help prioritize the deployment of limited suppression resources
546 (Roberto Barbosa et al., 2010; Mazzeo et al., 2022). The FPA FOD-Attributes dataset also
547 could be used in collaborative planning of forest restoration or fuel treatments. In cases
548 where ideas about prioritization of resources and assets for fire prevention efforts conflict
549 (Butler et al., 2015), robust scientific data such as the FPA FOD-Attribute dataset can help
550 facilitate a consensus (Colavito, 2017).

551 A rigorous quality assurance and quality check process was applied to the original FPA FOD
552 dataset, but some uncertainties remain. For example, some smaller fires are overseen by local
553 jurisdictions that may not have reporting standards as strict as those of federal firefighting
554 agencies (Short, 2014). The quality assurance process checks for duplicate fire records, but it
555 is possible that some duplicates remain due to the potential for multiple responding agencies
556 to record different information on the same fire. There is also uncertainty associated with
557 reported ignition locations. As a prerequisite for inclusion in the FPA FOD, a fire record's
558 geographic location must be at least as precise as a Public Land Survey System section,
559 which covers one square mile. In addition, the locations of many smaller fires overseen by
560 local jurisdictions may reflect the reporting location rather than the ignition location. For a
561 full description of the fire selection process for the FPA FOD and potential uncertainty, see
562 (Short, 2014). The FPA FOD-Attributes dataset does not provide details about large fire

563 growth days that may have occurred days to weeks from the ignition date, and interested
564 readers are encouraged to pair this dataset with the “all-hazards dataset” of (St. Denis et al.,
565 2023) for studies that focus on fire growth rates and intense fire behavior. Furthermore, the
566 current version of FPA FOD-Attributes dataset does not directly support analysis of
567 secondary fire impacts such as wildfire emissions and smoke that impact downwind
568 communities (Fowler et al., 2019).

569 Human ignition processes and wildfire impacts are prime areas for extensive new research,
570 and the FPA FOD-Attributes dataset is an initial effort to facilitate such knowledge
571 development. The FPA FOD-Attributes dataset also merits refinements and additions that
572 would further enhance its utility. For example, some of the socioeconomic variables (GDP,
573 population) are based on coarse scale information gathered through international efforts, and
574 using finer scale data may enhance the accuracy of the fire attributes. Additional economic
575 data to include in future versions may cover personal income and the workforce, also
576 available at sub-state levels from the Department of Commerce. Refined and expanded data
577 could allow for more direct inferences that connect human-caused ignition processes to fire
578 activity (e.g., Prestemon and Butry, 2005; Aldersley et al., 2011; Abt et al., 2015).

579 Although the entire FPA FOD-Attributes dataset is available in CSV format, the file is large
580 (over 4 GB). Therefore, advanced computing resources are necessary to work with the data.
581 To obtain a data file that is a more manageable size, the dataset can be filtered by attributes,
582 time period, or locations from the web portal (<https://fpafod.boisestate.edu/>) prior to
583 downloading.

584

585 **Data availability**

586 The FPA FOD-Attributes dataset, for 1992-2020 and for individual years, is available
587 through <https://zenodo.org/record/8381129> (DOI: 10.5281/zenodo.8381129) (Pourmohamad
588 et al. 2023)

589 The FPA FOD-Attributes dataset can be visualized and downloaded through
590 <https://fpafod.boisestate.edu>

591 Source data used to develop FPA FOD-Attributes are listed in Table S1.

592

593 **Code availability**

594 All codes that compiled FPA FOD-Attributes were developed in python and are available
595 through the FPA FOD-Attributes Github repository:
596 <https://github.com/YavarPourmohamad/FPA-FOD.git>

597 **Author contribution:**

598 Conceptualization: YP, MS, JTA
599 Methodology: YP, MS, JTA, EF, EJB, KS, MCR, NN, JPP
600 Software: YP, SB, EH
601 Validation: YP, JTA, MS, EJB, JO
602 Formal analysis: YP
603 Investigation: YP, MS, JTA
604 Resources: YP, MS, JTA, EF, EJB, KS, MCR, NN, AA
605 Data Curation: YP
606 Writing - Original Draft: MS, YP, JTA, EF, JO, PEH, AA, NN, JPP, KS, MCR
607 Visualization: YP, MS
608 Supervision: MS, JTA
609 Project administration: MS
610 Funding acquisition: MS, JTA

611

612 **Competing interests:**

613 The authors declare that they have no conflict of interest.

614 **Acknowledgments**

615 This study was supported by the Joint Fire Science Program (U.S. Department of the
616 Interior/Bureau of Land Management) grant number L21AC10247. The authors appreciate
617 the contributions of David Adams, Benjamin Collins, Brenden Marks, Jeremy Stocking,
618 Samuel Wasko, Ethan Raygor, and Parker Balbach to the development of the dataset portal:
619 <https://fpafod.boisestate.edu>

620

621 **References**

622 Abatzoglou, J. T.: Development of gridded surface meteorological data for ecological applications
623 and modelling, *Int. J. Climatol.*, 33, 121–131, 2013.

624 Abt, K. L., Butry, D. T., Prestemon, J. P., and Scranton, S.: Effect of fire prevention programs on
625 accidental and incendiary wildfires on tribal lands in the United States, *Int. J. Wildl. Fire*, 24, 749–762,
626 2015.

627 Aldersley, A., Murray, S. J., and Cornell, S. E.: Global and regional analysis of climate and human
628 drivers of wildfire, *Sci. Total Environ.*, 409, 3472–3481, 2011.

629 Alizadeh, M. R., Abatzoglou, J. T., Luce, C. H., Adamowski, J. F., Farid, A., and Sadegh, M.:
630 Warming enabled upslope advance in western US forest fires, *Proc. Natl. Acad. Sci. U. S. A.*, 118,
631 <https://doi.org/10.1073/pnas.2009717118>, 2021.

632 Alizadeh, M. R., Abatzoglou, J. T., Adamowski, J., Modaresi Rad, A., AghaKouchak, A., Pausata, F.

- 633 S. R., and Sadegh, M.: Elevation-dependent intensification of fire danger in the western United
634 States, *Nat. Commun.*, 14, 1773, 2023.
- 635 Balch, J. K., Bradley, B. A., Abatzoglou, J. T., Chelsea Nagy, R., Fusco, E. J., and Mahood, A. L.:
636 Human-started wildfires expand the fire niche across the United States, *Proc. Natl. Acad. Sci. U. S.*
637 *A.*, 114, 2946–2951, <https://doi.org/10.1073/pnas.1617394114>, 2017.
- 638 Barros, A. M. G., Day, M. A., Preisler, H. K., Abatzoglou, J. T., Krawchuk, M. A., Houtman, R., and
639 Ager, A. A.: Contrasting the role of human-and lightning-caused wildfires on future fire regimes on a
640 Central Oregon landscape, *Environ. Res. Lett.*, 16, 64081, 2021.
- 641 Bowman, D. M. J. S., Balch, J. K., Artaxo, P., Bond, W. J., Carlson, J. M., Cochrane, M. A.,
642 D'Antonio, C. M., DeFries, R. S., Doyle, J. C., and Harrison, S. P.: Fire in the Earth system, *Science*
643 (80-.), 324, 481–484, 2009.
- 644 Bowman, D. M. J. S., Balch, J., Artaxo, P., Bond, W. J., Cochrane, M. A., D'antonio, C. M., DeFries,
645 R., Johnston, F. H., Keeley, J. E., and Krawchuk, M. A.: The human dimension of fire regimes on
646 Earth, *J. Biogeogr.*, 38, 2223–2236, 2011.
- 647 Butler, W. H., Monroe, A., and McCaffrey, S.: Collaborative implementation for ecological restoration
648 on US public lands: implications for legal context, accountability, and adaptive management, *Environ.*
649 *Manage.*, 55, 564–577, 2015.
- 650 Flanagan, B.E., Hallisey, E.J., Adams, E. and Lavery, A.: Measuring community vulnerability to
651 natural and anthropogenic hazards: the Centers for Disease Control and Prevention's Social
652 Vulnerability Index. *Journal of Environ Health*, 80, 34-36, 2018, last access:
653 https://www.atsdr.cdc.gov/placeandhealth/svi/data_documentation_download.html [16 October 2023].
- 654 Chen, B. and Jin, Y.: Spatial patterns and drivers for wildfire ignitions in California, *Environ. Res.*
655 *Lett.*, 17, <https://doi.org/10.1088/1748-9326/ac60da>, 2022.
- 656 Chuvieco, E., Aguado, I., Salas, J., García, M., Yebra, M., and Oliva, P.: Satellite remote sensing
657 contributions to wildland fire science and management, *Curr. For. Reports*, 6, 81–96, 2020.
- 658 Cohen, J. D. and Deeming, J. E.: The National Fire Danger Rating System: Basic Equations (General
659 Technical Report PSW-GTR-82), US Dep. Agric. For. Serv. Berkeley, CA, USA, 1985.
- 660 Colavito, M. M.: The role of science in the collaborative forest landscape restoration program, *J. For.*,
661 115, 34–42, 2017.
- 662 Wildland Fire Executive Council. 2013. The National Cohesive Wildland Fire Management Strategy:
663 Phase III Western Regional Action Plan. 99 p. Available at: <https://www.frames.gov/catalog/14351>,
664 Accessed on 5/1/2024.
- 665 Dahal, D., Pastick, N. J., Boyte, S. P., Parajuli, S., Oimoen, M. J., & Megard, L. J.: Multi-Species
666 Inference of Exotic Annual and Native Perennial Grasses in Rangelands of the Western United
667 States Using Harmonized Landsat and Sentinel-2 Data. *Remote Sensing*, 14(4), 807.
668 <https://doi.org/10.3390/rs14040807>, 2022, Database access:
669 <https://data.usgs.gov/datacatalog/data/USGS:61716970d34ea36449a77130> [16 October 2023]
- 670 St. Denis, L. A., Short, K. C., McConnell, K., Cook, M. C., Mietkiewicz, N. P., Buckland, M., and
671 Balch, J. K.: all-hazards dataset mined from the US National Incident Management System 1999–
672 2020, *Sci. data*, 10, 112, 2023.
- 673 Dennison, P. E., Brewer, S. C., Arnold, J. D., and Moritz, M. A.: Large wildfire trends in the western
674 United States, 1984–2011, *Geophys. Res. Lett.*, 41, 2928–2933, 2014.
- 675 Dewitz, J.: National land cover database (NLCD) 2016 products, US Geol. Surv. data release, 10,
676 P96HHBIE, 2019.

- 677 Didan, K.: MODIS/Terra Vegetation Indices 16-Day L3 Global 1km SIN Grid V061 [Data set]. NASA
678 EOSDIS Land Processes Distributed Active Archive Center. last access: 16 October 2023,
679 <https://doi.org/10.5067/MODIS/MOD13A2.061>, 2021.
- 680 Dissing, D. and Verbyla, D. L.: Spatial patterns of lightning strikes in interior Alaska and their relations
681 to elevation and vegetation, *Can. J. For. Res.*, 33, 770–782, 2003.
- 682 Douglas, J., Mills, T. J., Artly, D., Ashe, D., Bartuska, A., Black, R. L., Coloff, S., Cruz, J., Edrington,
683 M., and Edwardson, J.: Review and update of the 1995 federal wildland fire management policy, US
684 Dept. of the Interior; US Dept. of Agriculture, 2001.
- 685 Eidenshink, J., Schwind, B., Brewer, K., Zhu, Z.-L., Quayle, B., and Howard, S.: A project for
686 monitoring trends in burn severity, *Fire Ecol.*, 3, 3–21, 2007.
- 687 Colorado Encyclopedia: East Troublesome Fire: [https://coloradoencyclopedia.org/article/east-](https://coloradoencyclopedia.org/article/east-troublesome-fire)
688 [troublesome-fire](https://coloradoencyclopedia.org/article/east-troublesome-fire), last access: 10 December 2023.
- 689 Finney, M. A., McHugh, C. W., Grenfell, I. C., Riley, K. L., and Short, K. C.: A simulation of
690 probabilistic wildfire risk components for the continental United States, *Stoch. Environ. Res. Risk*
691 *Assess.*, 25, 973–1000, 2011.
- 692 Flannigan, M. D. and Wotton, B. M.: Lightning-ignited forest fires in northwestern Ontario, *Can. J.*
693 *For. Res.*, 21, 277–287, 1991.
- 694 Fowler, M., Rad, A. M., Utych, S., Adams, A., Alamian, S., Pierce, J., Dennison, P., Abatzoglou, J. T.,
695 AghaKouchak, A., and Montrose, L.: A dataset on human perception of and response to wildfire
696 smoke, *Sci. data*, 6, 1–10, 2019.
- 697 Fuquay, D. M., Baughman, R. G., Latham, D. J.: A model for predicting lightning fire ignition in
698 wildland fuels, Intermountain Forest and Range Experiment Station, Forest Service, US, Wildfires,
699 Paper 5, https://digitalcommons.usu.edu/govdocs_wfires/5, 1979.
- 700 Hély, C., Flannigan, M., Bergeron, Y., and McRae, D.: Role of vegetation and weather on fire
701 behavior in the Canadian mixedwood boreal forest using two fire behavior prediction systems, *Can. J.*
702 *For. Res.*, 31, 430–441, 2001.
- 703 Hessilt, T. D., Abatzoglou, J. T., Chen, Y., Randerson, J. T., Scholten, R. C., Van Der Werf, G., and
704 Veraverbeke, S.: Future increases in lightning ignition efficiency and wildfire occurrence expected
705 from drier fuels in boreal forest ecosystems of western North America, *Environ. Res. Lett.*, 17,
706 <https://doi.org/10.1088/1748-9326/ac6311>, 2022.
- 707 Houtman, R. M., Montgomery, C. A., Gagnon, A. R., Calkin, D. E., Dietterich, T. G., McGregor, S.,
708 and Crowley, M.: Allowing a wildfire to burn: estimating the effect on future fire suppression costs, *Int.*
709 *J. Wildl. Fire*, 22, 871–882, 2013.
- 710 Huete, A., Didan, K., Miura, T., Rodriguez, E. P., Gao, X., and Ferreira, L. G.: Overview of the
711 radiometric and biophysical performance of the MODIS vegetation indices, *Remote Sens. Environ.*,
712 83, 195–213, 2002.
- 713 Iglesias, V., Balch, J. K., and Travis, W. R.: US fires became larger, more frequent, and more
714 widespread in the 2000s, *Sci. Adv.*, 8, eabc0020, 2022.
- 715 Kennedy, C. M., Oakleaf, J. R., Theobald, D. M., Baruch-Mordo, S., and Kiesecker, J.: Managing the
716 middle: A shift in conservation priorities based on the global human modification gradient, *Glob.*
717 *Chang. Biol.*, 25, 811–826, 2019.
- 718 Khorshidi, M. S., Dennison, P. E., Nikoo, M. R., AghaKouchak, A., Luce, C. H., and Sadegh, M.:
719 Increasing concurrence of wildfire drivers tripled megafire critical danger days in Southern California
720 between 1982 and 2018, *Environ. Res. Lett.*, 15, 104002, 2020.

- 721 Kummu, M., Taka, M., and Guillaume, J. H. A.: Gridded global datasets for gross domestic product
722 and Human Development Index over 1990–2015, *Sci. data*, 5, 1–15,
723 <https://doi.org/https://doi.org/10.5061/dryad.dk1j0>, 2018.
- 724 U.S. Department of Interior, Geological Survey, and U.S. Department of Agriculture: LANDFIRE
725 Existing Vegetation Type layer (2022, May - last update), <http://landfire.cr.usgs.gov/viewer/>, last
726 access: 16 October 2023.
- 727 U.S. Department of Interior, Geological Survey, and U.S. Department of Agriculture: LANDFIRE Fire
728 Regime Groups Type layer (2022, May - last update), <http://landfire.cr.usgs.gov/viewer/>, last access:
729 16 October 2023.
- 730 U.S. Department of Interior, Geological Survey, and U.S. Department of Agriculture: LANDFIRE
731 Topography Type layer (2022, May - last update), <http://landfire.cr.usgs.gov/viewer/>, last access: 16
732 October 2023.
- 733 Latham, D. and Williams, E.: Lightning and forest fires, in: *Forest Fires*, Elsevier, 375–418, 2001.
- 734 Maranghides, A., Link, E., Hawks, S., Wilson, M., Brewer, W., Brown, C., Vihnanek, B., and Walton,
735 W. D.: A Case Study of the Camp Fire–Fire Progression Timeline Appendix C. Community WUI Fire
736 Hazard Evaluation Framework, 2021.
- 737 Mazzeo, G., De Santis, F., Falconieri, A., Filizzola, C., Lacava, T., Lanorte, A., Marchese, F., Nolè,
738 G., Pergola, N., and Pietrapertosa, C.: Integrated Satellite System for Fire Detection and
739 Prioritization, *Remote Sens.*, 14, 335, 2022.
- 740 McGee, T., McFarlane, B., and Tymstra, C.: Wildfire: a Canadian perspective, in: *Wildfire hazards,*
741 *risks and disasters*, Elsevier, 35–58, 2015.
- 742 Meisner, B. N., Chase, R. A., McCutchan, M. H., Mees, R., Benoit, J. W., Ly, B., Albright, D., Strauss,
743 D., and Ferryman, T.: A lightning fire ignition assessment model, in: *12th Conference on Fire and*
744 *Forest Meteorology*. Jekyll Island, GA, 172–178, 1993.
- 745 Miller, C. and Ager, A. A.: A review of recent advances in risk analysis for wildfire management, *Int. J.*
746 *Wildl. fire*, 22, 1–14, 2012.
- 747 Modaresi Rad, A., Abatzoglou, J. T., Kreitler, J., Alizadeh, M. R., AghaKouchak, A., Hudyma, N.,
748 Nauslar, N. J., and Sadegh, M.: Human and infrastructure exposure to large wildfires in the United
749 States, *Nat. Sustain.*, 1–9, 2023.
- 750 Wildland fire perimeters full history: [https://data-nifc.opendata.arcgis.com/datasets/nifc::wfigs-](https://data-nifc.opendata.arcgis.com/datasets/nifc::wfigs-wildland-fire-perimeters-full-history/explore)
751 [wildland-fire-perimeters-full-history/explore](https://data-nifc.opendata.arcgis.com/datasets/nifc::wfigs-wildland-fire-perimeters-full-history/explore), last access: 26 February 2023.
- 752 Nguyen, D., Belval, E. J., Wei, Y., Short, K. C., and Calkin, D. E.: Dataset of United States Incident
753 Management Situation Reports, 2007-2021, *Sci. Data*, 2023.
- 754 Noonan-Wright, E. K., Opperman, T. S., Finney, M. A., Zimmerman, G. T., Seli, R. C., Elenz, L. M.,
755 Calkin, D. E., and Fiedler, J. R.: Developing the US wildland fire decision support system, *J.*
756 *Combust.*, 2011, 2011.
- 757 Pineda, N., Altube, P., Alcasena, F. J., Casellas, E., Segundo, H. S., and Montanyà, J.:
758 Characterising the holdover phase of lightning-ignited wildfires in Catalonia, *Agric. For. Meteorol.*,
759 324, <https://doi.org/10.1016/j.agrformet.2022.109111>, 2022.
- 760 Pourmohamad, Y., Abatzoglou, J., Belval, E., Short, K., Fleishman, E., Reeves, M., Nauslar, N.,
761 Higuera, P., Henderson, E., Ball, S., AghaKouchak, A., Prestemon, J., Olszewski, J., and Sadegh, M.
762 Physical, Social, and Biological Attributes for Improved Understanding and Prediction of Wildfires:
763 FPA FOD-Attributes Dataset (1.0) [Data set]. Zenodo. <https://doi.org/10.5281/zenodo.8381129>, 2023.

- 764 Prestemon, J. P. and Butry, D. T.: Time to burn: modeling wildland arson as an autoregressive crime
765 function, *Am. J. Agric. Econ.*, 87, 756–770, 2005.
- 766 Climate and Economic Justice Screening Tool: <https://screeningtool.geoplatform.gov/>, last access: 10
767 December 2023.
- 768 Rad, A. M., Abatzoglou, J., Fleishman, E., Mockrin, M. H., Radeloff, V. C., Pourmohamad, Y., Cattau,
769 M. E., Johnson, J. M., Higuera, P. E., Nauslar, N., and Sadegh, M.: Social vulnerability of the people
770 exposed to wildfires, *Sci. Adv.*, 9, eadh461, 2023.
- 771 Reeves, M. and Frid, L.: The Rangeland Vegetation Simulator: A user-driven system for quantifying
772 production, succession, disturbance and fuels in non-forest environments, in: 10th International
773 Rangeland Congress, 1062, 2016.
- 774 Reeves, M. C., Hanberry, B. B., Wilmer, H., Kaplan, N. E., and Lauenroth, W. K.: An assessment of
775 production trends on the Great Plains from 1984 to 2017, *Rangel. Ecol. Manag.*, 78, 165–179, 2021.
- 776 Riley, S. J., DeGloria, S. D., and Elliot, R.: Index that quantifies topographic heterogeneity, *Intermt. J.*
777 *Sci.*, 5, 23–27, 1999.
- 778 Roberto Barbosa, M., Carlos Sícoli Seoane, J., Guimarães Buratto, M., Santana de Oliveira Dias, L.,
779 Paulo Carvalho Raivel, J., and Lobos Martins, F.: Forest Fire Alert System: a Geo Web GIS
780 prioritization model considering land susceptibility and hotspots—a case study in the Carajás National
781 Forest, Brazilian Amazon, *Int. J. Geogr. Inf. Sci.*, 24, 873–901, 2010.
- 782 Ronchi, E., Gwynne, S. M. V., Rein, G., Wadhvani, R., Intini, P., and Bergstedt, A.: e-Sanctuary:
783 Open multi-physics framework for modelling wildfire urban evacuation, Fire Protection Research
784 Foundation Quincy, 2017.
- 785 Rothberg, D.: “It’s gone, it’s gone:” Nation’s largest wildfire in Nevada devastates ranches, sage
786 grouse, *Nevada Indep.*, 12th July, 2018.
- 787 Rouse, J. W., Haas, R. H., Schell, J. A., and Deering, D. W.: Monitoring vegetation systems in the
788 Great Plains with ERTS, *NASA Spec. Publ.*, 351, 309, 1974.
- 789 Santos, F., Bailey, J. K., and Schweitzer, J. A.: The eco-evolutionary role of fire in shaping terrestrial
790 ecosystems, *Functional Ecology*, 37, 2090-2095, 2023.
- 791 Scott, J., Helmbrecht, D., Thompson, M. P., Calkin, D. E., and Marcille, K.: Probabilistic assessment
792 of wildfire hazard and municipal watershed exposure, *Nat. Hazards*, 64, 707–728, 2012.
- 793 Short, K. C.: A spatial database of wildfires in the United States, 1992-2011, *Earth Syst. Sci. Data*, 6,
794 1–27, <https://doi.org/10.5194/essd-6-1-2014>, 2014.
- 795 Short, K. C.: Spatial wildfire occurrence data for the United States, 1992-2018
796 [FPA_FOD_20210617], 2021.
- 797 Short, K. C.: Spatial wildfire occurrence data for the United States, 1992-2020
798 [FPA_FOD_20221014], 2022.
- 799 Short, K. C., Grenfell, I. C., Riley, K. L., and Vogler, K. C.: Pyromes of the conterminous United
800 States, Forest Service Research Data Archive, <https://doi.org/10.2737/RDS-2020-0020>, 2020.
- 801 Show, S. B. and Kotok, E. I.: Forest fires in California, 1911-1920: an analytical study, 1923.
- 802 Shuman, J. K., Balch, J. K., Barnes, R. T., Higuera, P. E., Roos, C. I., Schwilk, D. W., Stavros, E. N.,
803 Banerjee, T., Bela, M. M., and Bendix, J.: Reimagine fire science for the anthropocene, *PNAS Nexus*,
804 1, pgac115, 2022.

805 Silva, F. R. y, O'Connor, C. D., Thompson, M. P., Martinez, J. R. M., and Calkin, D. E.: Modelling
806 suppression difficulty: current and future applications (vol 29, pg 781, 2020), *Int. J. Wildl. FIRE*, 29,
807 752, 2020.

808 Stephens, S. L., Agee, J. K., Fule, P. Z., North, M. P., Romme, W. H., Swetnam, T. W., and Turner,
809 M. G.: Managing forests and fire in changing climates, *Science* (80-.), 342, 41–42, 2013.

810 Tatem, A. J.: WorldPop, open data for spatial demography, *Sci. data*, 4, 1–4, 2017.

811 Omernik, J.M. Ecoregions of the conterminous United States. *Annals of the Association of American*
812 *Geographers* 77:118-125, Available at:
813 https://gaftp.epa.gov/EPADDataCommons/ORD/Ecoregions/us/us_eco_l4_state_boundaries.zip, last
814 access: 10 December 2023, 1987.

815 Home Land Security: Fire Stations,
816 [https://opendata.arcgis.com/api/v3/datasets/0ccaf0c53b794eb8ac3d3de6afdb3286_0/downloads/dat](https://opendata.arcgis.com/api/v3/datasets/0ccaf0c53b794eb8ac3d3de6afdb3286_0/downloads/data?format=shp&spatialRefId=3857&where=1%3D1)
817 [a?format=shp&spatialRefId=3857&where=1%3D1](https://opendata.arcgis.com/api/v3/datasets/0ccaf0c53b794eb8ac3d3de6afdb3286_0/downloads/data?format=shp&spatialRefId=3857&where=1%3D1), last access: 13 March 2023.

818 U.S. Geological Survey (USGS) Gap Analysis Project (GAP): Protected Areas Database of the
819 United States (PAD-US) 3.0: U.S. Geological Survey data release,
820 <https://doi.org/10.5066/P9Q9LQ4B>, 2022.

821 TIGER: US Census Roads: [https://www.census.gov/geographies/mapping-files/time-series/geo/tiger-](https://www.census.gov/geographies/mapping-files/time-series/geo/tiger-line-file.2022.html#list-tab-790442341)
822 [line-file.2022.html#list-tab-790442341](https://www.census.gov/geographies/mapping-files/time-series/geo/tiger-line-file.2022.html#list-tab-790442341), last access: 16 October 2023.

823 Vermote, E.: NOAA Climate Data Record (CDR) of AVHRR normalized difference vegetation index
824 (NDVI), version 5. NOAA National Centers for Environmental Information,
825 <https://doi.org/https://doi.org/10.7289/V5ZG6QH9>, 2019.

826 Viegas, D. X., Viegas, M., and Ferreira, A. D.: Moisture content of fine forest fuels and fire occurrence
827 in central Portugal, *Int. J. Wildl. Fire*, 2, 69–86, 1992.

828 Weaver, J. F., Lindsey, D., Bikos, D., Schmidt, C. C., and Prins, E.: Fire detection using GOES rapid
829 scan imagery, *Weather Forecast.*, 19, 496–510, 2004.

830 Weiss, A.: Topographic position and landforms analysis, in: Poster presentation, ESRI user
831 conference, San Diego, CA, 2001.

832 Westerling, A. L.: Increasing western US forest wildfire activity: sensitivity to changes in the timing of
833 spring, *Philos. Trans. R. Soc. B Biol. Sci.*, 371, 20150178, 2016.

834 Wierzchowski, J., Heathcott, M., and Flannigan, M. D.: Lightning and lightning fire, central cordillera,
835 Canada, *Int. J. Wildl. Fire*, 11, 41–51, 2002.

836 WorldPop: Global high resolution population denominators project, Funded by Bill Melinda Gates
837 Found. Sch. Geogr. Environ. Sci. Univ. Southampton; Dep. Geogr. Geosci. Univ. Louisville; Dep.
838 Geogr. Univ. Namur) Cent. Int. Earth Sci. Inf. Netw.(CIESIN), Columbia Univ, 2018.

839 Silva, F. R., Martínez, J. R. M., and González-Cabán, A.: A methodology for determining operational
840 priorities for prevention and suppression of wildland fires, *Int. J. Wildl. fire*, 23, 544–554, 2014.

841 Silva, F. R., O'Connor, C. D., Thompson, M. P., Martínez, J. R. M., and Calkin, D. E.: Corrigendum
842 to: Modelling suppression difficulty: current and future applications, *Int. J. Wildl. fire*, 29, 752, 2020.

843